Microstructure of Dilute Hydrophobically Modified Alkali Soluble Emulsion in Aqueous Salt Solution

S. Dai,[†] K. C. Tam,*[,†] and R. D. Jenkins[‡]

School of Mechanical and Production Engineering, Nanyang Technological University, Nanyang Avenue, Singapore 639798, Republic of Singapore, and Union Carbide Asia Pacific Inc., Technical Center, 16 Science Park Drive, The Pasteur, Singapore 118227, Republic of Singapore

Received June 3, 1999; Revised Manuscript Received October 19, 1999

ABSTRACT: The microstructure of a model HASE associative polymer in aqueous salt solution is complex and has not been defined until now. On the basis of the results from static and dynamic light scattering studies, a physical model describing the microstructure of a model HASE polymer in aqueous salt solution is proposed. The model HASE polymer contains a copolymer backbone of equal moles of methacrylic acid (MAA) and ethyl acrylate (EA) with 1 mol % of $C_{16}H_{33}$ hydrophobic modified macromonomer distributed randomly along the backbone. In very dilute aqueous solutions (0.005−0.1 wt %), two decay modes are observed in the relaxation time distribution function. The fast and the slow modes correspond to the translational diffusion of the unimers and the polymer aggregates (consisting of about five polymer chains), respectively. The polymer aggregate is formed by association of the hydrophobic macromonomer via a closed association mechanism. When the polymer concentration increases, the polymer aggregates grow in size. The fractal dimension, d_f, decreases with increasing polymer concentrations, indicating that the aggregates are becoming less compact. At the same time, when the polymer concentration exceeds 0.1 wt %, the unimers are transformed to oligomers consisting of two or more polymer chains.

Introduction

Associative polymers are a class of macromolecules with attractive groups or "stickers" either attached at the ends (telechelic system) or distributed along the backbone (combed system). This class includes charged polymers (ionomers, polyelectrolytes, and polyampholytes), block copolymers in strongly selective solvents, and polymers with hydrogen bonding.[1] They are widely used in a number of applications such as rheology modifiers, adhesives, adsorbents, coatings, biomedical implants, flocculent for wastewater treatment, surfactant and stabilizers for heterogeneous polymerization, and suspending agents for pharmaceutical delivery systems.[2,3] One typical example of associative polymers is the aqueous solutions of block copolymers. These associative polymers usually contain a water-soluble hydrophilic backbone and insoluble hydrophobic groups located at the ends of the polymer chain or distributed along the polymer backbone. When the polymer dissolves in water, clusters of hydrophobic domains are formed, yielding a network structure. Such structure induces a large increase in the solution viscosity, producing a viscous and often elastic and gellike fluid behavior. Hence, associative polymers are good candidates for thickening agents in environmentally friendly coating applications. Interests in this field have increased, and fundamental studies on such a polymer system have become an active research area in the past two decades.[4−16]

HASE (hydrophobically modified alkali soluble emulsion) is among one of many varieties of new generations of synthetic associative thickeners. It has a structure resembling that of a combed-like polymer.[17] This thickener contains a copolymer backbone consisting of methacrylic acid and ethyl acrylate. A small proportion (usually 1−3 mol %) of hydrophobic groups with a short poly(ethylene oxide) hydrophilic segment are attached to the hydrophilic backbone via an unsaturated isocyanate linkage. When the polymer is dissolved in an alkali media, the backbone becomes hydrophilic and the latex emulsion dissolves. In aqueous solutions, these hydrophobic groups associate and form clusters through the intra- and intermolecular interactions. If the polymer concentration is greater than a critical value, a transient network structure is formed, which gives rise to the dramatic increase in the solution viscosity. Up to now, the microstructure and the association mechanism of these polymers in aqueous solutions is still unclear. Many techniques, such as fluorescence spectroscopy, pulse gradient NMR, dynamic light scattering, and rheology, can be used to investigate the behavior of the HASE polymer in aqueous solution. Several publications on the rheological properties and the fluorescence spectroscopy of this thickener have been reported.[18−28]

In this paper, both static and dynamic light scattering were used to study the microscopic conformation and the association mechanism of a model HASE polymer in aqueous salt solution. The chemical structure of this HASE, designated as HASE-35EO-16C, is shown in Figure 1. The effects of temperature, ionic strength, and pH are described elsewhere.[29] All the measurements here were carried out at 298 K, pH 9, in 0.1 M NaCl aqueous solutions. At pH of 9, complete neutralization of the methacrylic acid is achieved, while with 0.1 M NaCl, electrostatic interactions between charges along the polymer backbone are minimized. The polymer concentration was varied from 0.005 to 0.408 wt %.

Materials and Methods

Samples and Sample Preparation. The HASE copolymer, designated as HASE-35EO-16C, was synthesized by

[†] Nanyang Technological University.
[‡] Union Carbide Asia Pacific Inc.
* To whom the corresponding should be addressed. Currently on sabbatical leave at the Department of Mechanical Engineering, MIT. e-mail mkctam@ntu.edu.sg; FAX (65) 791-1859.

10.1021/ma990887n CCC: $19.00
Published on Web 12/28/1999

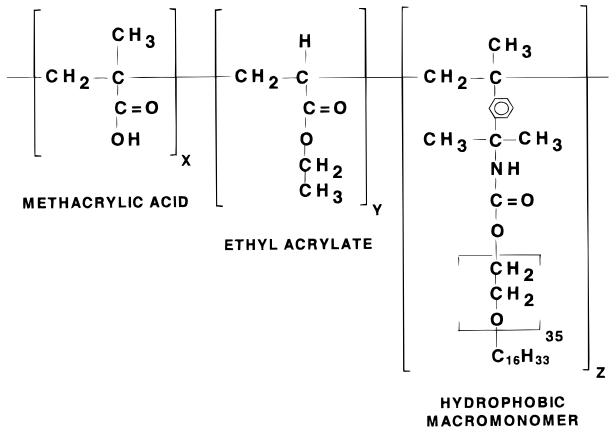

Figure 1. Chemical structure of HASE-35EO-16C.

Union Carbide. The emulsion copolymerized product contains 50 mol % methacrylic acid (MAA), 49 mol % ethyl acrylate (EA), and 1 mol % $C_{16}H_{33}$ macromonomer. The details of synthesis and characterization of the polymer were described elsewhere.[18,21] The hexadecyl group was ethoxylated with ~35 mol of ethylene oxide.

The HASE-35EO-16C in latex form was dialyzed using a cellulose membrane placed in the Millipore deionized water for about 4 weeks, with a weekly change of water. The cellulose dialysis membrane removes molecules with M_w below 14 000. After dialysis, the clean latex concentration was determined by drying in the vacuum oven at 80−100 °C. The stock solution was prepared at a concentration of 1 wt % total polymer in deionized water and kept in the refrigerator at a temperature of ~ 6 °C. Other reagents, such as NaCl and AMP (2-amino-2-methylpropanol-1) was used as received. The samples were diluted from that stock solution using 0.2 M NaCl aqueous solution and filtered deionized water. AMP was used to adjust the pH to approximately 9. Measurements were performed after 24 h to ensure that an equilibrium microstructure was attained. Prior to conducting the light scattering measurement, the sample solutions were filtered through a 0.2 μm filter to remove any dust particles that may be present in the test solution.

Equipment. The Brookhaven BI-200SM goniometer system equipped with a 522-channel BI9000AT digital multiple τ correlator was used to perform the light scattering experiments. The light source is a power adjustable vertical polarized argon ion laser with the wavelength of 488 nm. The measured temperature was controlled at 25 ± 0.1 °C using a Science/Electronic water bath. The REPES inverse Laplace transform (ILT) routine supplied with the GENDIST software package[30] was used to analyze the intensity−intensity autocorrelation functions. The probability of reject was set to 0.5.

Rheological measurements of dilute polymer solutions were carried out using the Contraves LS40 controlled rate rheometer. The rheometer was fitted with the MS41S/1S concentric cylinder measuring system consisting of a cup with diameter of 12 mm and a bob with the diameter of 11 mm and the height of 8 mm.

Results and Discussions

Static Light Scattering. Static light scattering is a conventional method for determining the weight-averaged molecular weight (M_w) of polymers. From the static light scattering, the second virial coefficient (A_2) and the z-averaged radius of gyration (R_g) can be determined.[31,32] If the particle size is larger than $\lambda_0/20$, the basic relation for static light scattering is

$$\frac{KC}{R_\theta} = \left(\frac{1}{M_w} + 2A_2C\right)\left(1 + \frac{q^2R_g^2}{3}\right) \qquad (1)$$

where K ($=4\pi n_0^2(\mathrm{d}n/\mathrm{d}C)^2/N_A\lambda_0^4$) is an optical constant

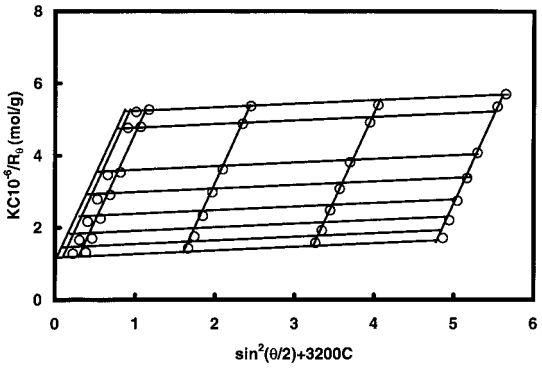

Figure 2. Static light scattering (Zimm plot) of dilute HASE-35EO-16C in 0.1 M NaCl aqueous solutions at pH 9, 298 K. (Angles range from 30° to 135°; concentrations range from 0.005 to 0.15 wt %.)

with N_A, n_0, and λ_0 being Avogadro's number, the solvent refractive index, and the wavelength of the light in a vacuum, respectively. C is the polymer concentration in grams per milliliter, and R_θ is the excess Rayleigh ratio at scattering angle θ with vertically polarized incident and scattered beams. The scattering vector, $\mathbf{q}$ ($=4\pi n \sin(\theta/2)/\lambda$), is defined as the difference between the scattered beam and the incident beam. The refractive index increment of the polymer solutions ($\mathrm{d}n/\mathrm{d}c$) can be measured using a differential refractometer.

A Zimm plot is always used to analyze the static light scattering data. Figure 2 shows the Zimm plot of dilute HASE-35EO-16C in 0.1 M NaCl at 298 K, pH 9. The measurement yields an apparent weight-averaged molecular weight of 9.9×10^5g/mol, an apparent second virial coefficient of 1.15×10^{-4} (cm^3 mol)/g and an apparent radius of gyration of 114 nm. Because of hydrophobic associations, it is difficult to determine the molecular weight and molecular weight distribution of single polymer chain. We found that both organic solvents and cosolvents do not completely remove the hydrophobic association. At the same time, cleaving the hydrophobes by hydrolysis reaction and the shielding of hydrophobic associations using surfactants alters the polymer structure. The determination of the molecular weight and MW distribution of HASE polymer is a challenging and difficult task. However, Ou-Yang and co-workers[33] recently reported the MW and MWD of single polymer chains. They removed the association using β-cyclodextrin, and the M_W of the nonassociated chain was found to be between 200 000 and 250 000. The molecular weight distribution of individual polymer chain is not broad. Comparison of our results and that of Ou-Yang and co-workers suggests that large aggregates or polymer clusters are present in aqueous solutions, even at extremely low polymer concentrations. By combining the static light scattering with the dynamic light scattering results, additional information on the large aggregates or clusters could be derived. This will be discussed later.

Fractal Dimension of Aggregates. In dilute solution, the excess scattering intensity of polymer molecules is related to the structure factor $S(q)$ and the form factor $P(q)$, i.e.

$$I(q) \propto S(q)\,P(q) \qquad (2)$$

$S(q)$ and $P(q)$ correspond to the space correlation between monomers of different polymer chains and that

Table 1. Summaries of Static and Dynamic Light Scattering Parameters for Dilute HASE-35EO-16C at pH 9 and 298 K, in 0.1 M NaCl Solutions

concn (wt %)	D_f (10^{11} m^2/s)	D_s (10^{12} m^2/s)	η (Pa s)	$D_f\eta/T$ (10^{17} N/K)	$D_s\eta/T$ (10^{17} N/K)	R_h[a] (unimer)	R_h[a] (aggregate)	R_h(agg)/R_h(u)	d_f
0.00493	1.27	3.12	0.001 02	4.34	1.07	19.3	78.7	4.1	2.34
0.00998	1.26	3.11	0.001 06	4.47	1.11	19.5	78.9	4.1	2.35
0.0265	1.30	3.03	0.001 05	4.57	1.07	18.9	81.0	4.3	2.35
0.0493	1.39	2.93	0.001 07	4.66	1.09	17.7	83.8	4.7	2.11
0.0804	1.50	2.83	0.001 07	5.39	1.02	16.4	86.7	5.3	2.01
0.0964	1.57	2.74	0.001 09	5.09	1.07	15.6	89.6	5.7	1.94
0.1459	1.54	2.59	0.001 12	5.65	1.06	15.9	94.7	5.9	1.76
0.1951	1.45	2.45	0.001 15	6.05	1.06	16.9	100.2	5.9	1.74
0.3057	1.27	2.18	0.001 19	6.15	1.03	19.3	112.6	5.8	1.54
0.4081	1.08	1.97	0.001 31	6.37	1.08	22.7[b]	124.6	5.5	1.33

[a] Apparent hydrodynamic radius. [b] Apparent hydrodynamic radius of oligomers.

of the same polymer chains, respectively.[34−36] At the condition of $qR_{g,u} < 1 < qR_{g,agg}$, the average intensity is related to q as shown:

$$I(q) \propto q^{-d_f} \tag{3}$$

$R_{g,u}$ and $R_{g,agg}$ are the radius of gyration of unimers and aggregates, respectively, and d_f is the static fractal dimension. The static fractal dimension can be used to indicate the kinetic process of aggregation and the compactness of the aggregates. The value of static fractal dimension is determined from a plot of ln $I(q)$ vs ln q.

One of the main conceptual theoretical frameworks used to describe aggregation process is the kinetic approach.[34,35] The kinetic approach gives a mean field description of aggregation processes when the positions of the aggregates are not correlated. Two well-studied limiting cases are the reaction-limited cluster−cluster aggregation (RLCA), where the sticking probability between particles tends to zero, and the diffusion-limited cluster−cluster aggregation (DLCA), where the sticking probability between particles tends to unity. For the DLCA cluster, the fractal dimension $d_f \sim 1.8$, while for the RLCA cluster, $d_f \sim 2.1$. Any interaction between parts of clusters in the docking process would make them deviate from the two motions described above. Meanwhile, at condition of $qR_{g,agg} > 1$,

$$M_{agg} \propto R_{g,agg}^{d_f} \tag{4}$$

where M_{agg} is the molecular weight of the aggregates. Hence, the larger the fractal dimension, the more compact the structure, and the lower the fractal dimension, the more open is the structure.[34,36]

The q dependence of the scattering intensity for HASE-35EO16C at different concentrations was used to investigate the compactness of the cluster and the aggregation process. The log−log relationship of intensities and scattering vector is shown in Figure 3. It is clear that the intensity decreases with increasing q, and the magnitude of the slope decreases with increasing polymer concentration. On the basis of the relationship described in eq 3, the slope in the log−log plot yields the value of d_f, which is summarized in Table 1. The magnitude of d_f remained almost constant at ~2.35 at concentration less than 0.05 wt %, and it decreases with increasing polymer concentration. The decrease in d_f with increasing polymer concentrations was also reported by Carpineti et al. on the aggregation of polystyrene.[35] The maximum d_f is 2.35 (which is larger than 2.1), suggesting that the aggregation process deviates from either the DLCA or the RLCA process. It may not

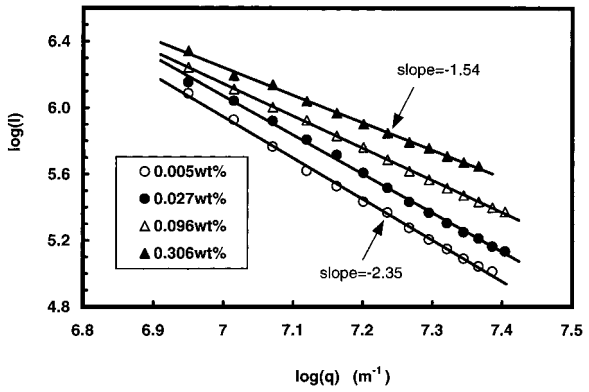

Figure 3. Plot of ln(I) versus ln(q) for the determination of static fractal dimension.

be feasible to use the simple mechanism of RLCA and DLCA to interpret the aggregation process of HASE polymer system. At the polymer concentration of less than 0.05 wt %, d_f remained constant, which suggests that the structure of the cluster does not change. However, d_f decreases at $c > 0.05$ wt %, indicating that the clusters become less compact at higher polymer concentration. The trends of the fractal dimension at varying polymer concentrations seem to correlate with the dynamic light scattering data.

Dynamic Light Scattering. Dynamic light scattering measures the temporal fluctuations of the scattered light produced by polymer molecules. The temporal variation of the scattered radiation yields the familiar Doppler shift, and the broadening of the central Rayleigh line can be used to determine the dynamic properties of the system. The intensity of the scattered light can be analyzed by photon correlation spectroscopy (PCS).[30,32,37]

The normalized intensity−intensity autocorrelation function is expressed as

$$g_2(t) = \frac{\langle I(t)\, I(t+\tau)\rangle}{\langle I(t)^2\rangle} \tag{5}$$

where $I(t)$ is an average value of the products of the scattered intensity at an arbitrary time, t, and $I(t+\tau)$ is the intensity registered at delay time τ. The above expression can be simplified using the Siegert relations

$$g_2(t) = 1 + \beta|g_1(t)|^2 \tag{6}$$

where β is the coherence factor and $g_1(t)$ is the field autocorrelation function, which is described by the expression

$$g_1(t) = \int w(\Gamma) \exp(-\Gamma t)\, d\Gamma \quad (7)$$

where $w(\Gamma)$ is a continuous distribution function of decay rate Γ; the decay rate is the inverse of the relaxation time τ. If the inverse Laplace transform (ILT) is used to analyze the autocorrelation functions, the relationship between $w(\Gamma)$ and Γ can be obtained. Meanwhile, for the translational diffusion mode, the decay rate is related to the translational diffusion coefficient D by

$$\Gamma = Dq^2 \quad (8)$$

and the Stokes−Einstein expression can be expressed as

$$D_0 = \frac{kT}{6\pi\eta_0 R_h} \quad (9)$$

where k is the Boltzmann constant, T the absolute temperature in kelvin, η_0 the solvent viscosity, R_h the hydrodynamic radius of polymer, and D_0 the translational diffusion coefficient at infinitely dilute concentration.

Angular Dependence. Dynamic light scattering measurements were carried out at different measurement angles. The autocorrelation functions and their respective time distribution functions of 0.005 wt % HASE-35EO16C in 0.1 M NaCl at pH 9, 298 K, are shown in Figure 4a,b. REPES was used to analyze the autocorrelation function. The figure indicates that the system contains two peaks in the relaxation time distribution. At low measurement angles, the two main peaks are fully separated. The peaks are assigned as the fast and the slow decay mode, respectively, and they can be represented by two characteristic relaxation times, τ_f and τ_s (where $\tau_f < \tau_s$). τ_f represents the relaxation time of the fast decay mode (the left peak). τ_s represents the relaxation time of the slow decay mode (the right peak). Meanwhile, the ratio of the two peaks, A_f/A_s, decreases as the measurement angle is decreased and reaches a minimum value of approximately 1/9. A_f/A_s represents the relative contribution to the intensity from these two components. From static light scattering results, the large apparent radius of gyration in the solution implies that large clusters exist in the polymer solution. For the large cluster, A_f/A_s is angle dependent because the smaller measurement angle is sensitive to large particles.

Figure 5 reveals the dependence of the decay rate on the scattering vector of 0.005 wt % HASE-35EO-16C solution. It is evident that both the fast and the slow modes are diffusion modes as Γ/q^2 is independent of the scattering vector, which implies that the decay rate is linearly dependent on q^2. The magnitude of the Γ/q^2 corresponds to the translational diffusion coefficient. The diffusion coefficients of dilute HASE-35EO-16C in 0.1 M NaCl solutions are summarized in Table 1. The fast mode represents the translational diffusion of individual polymer chain or unimer, while the slow mode is attributed to the translational diffusion of a larger aggregate or polymer cluster in the solution.[36] It is evident that all the peaks shift to the left as the measurement angles were increased. In some cases, the peaks merge, particularly at larger measurement angles due to the reduction in the distance of relaxation times between the two decay modes.

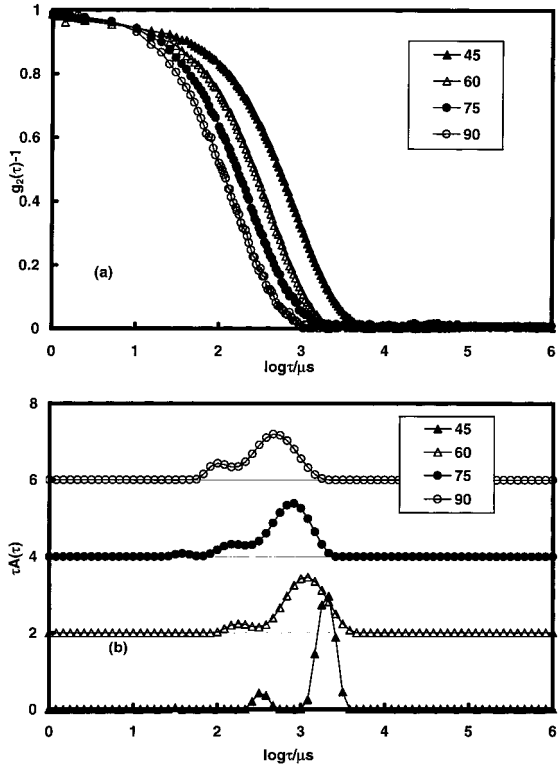

Figure 4. (a) Field autocorrelation function and (b) decay time distribution function of 0.005 wt % RDJ3501 in 0.1 M NaCl solution, at pH 9 and 298 K.

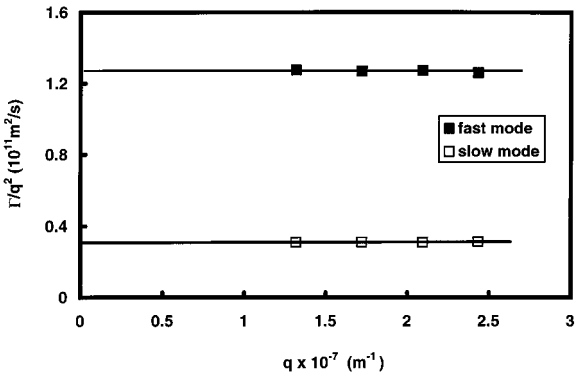

Figure 5. Relationship of Γ/q^2 and q for 0.005 wt % HASE-35EO-16C in 0.1 M NaCl solution, at pH 9 and 298 K.

If the relaxation process is caused by the translational diffusion movement of molecules, then the relaxation time and the scattering vector possess the following relationship, i.e., $\tau \propto 1/q^2$. For HASE polymer solutions, it is known that $\Gamma \propto \sin^2(\theta/2)$, i.e., $\tau \propto 1/\sin^2(\theta/2)$. This relation can be used to interpret the shifting of the peaks to the left when the measurement angle is increased. We define $\Delta\tau$ as the distance of relaxation time between two peaks at a given measurement angle, i.e., $\Delta\tau = \tau_s - \tau_f$. Since $\Delta\tau \propto [\sin^2(\theta/2)]^{-1}$ for $0 < \theta < 180°$, $[\sin^2(\theta/2)]^{-1}$ would decrease with increasing angle θ. Hence, the two peaks will merge as the measurement angles increase.

Aggregates in Polymer Solutions. Both the static and the dynamic light scattering results reveal that large aggregates or polymer clusters exist in the dilute polymer solutions. On the basis of the diffusion coefficients of large aggregates, the hydrodynamic particle size can be determined from the Einstein−Stokes equation, (eq 9). The apparent hydrodynamic size is about

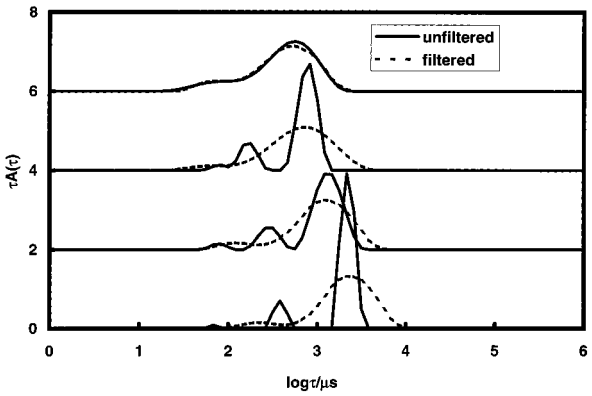

Figure 6. Comparison of 0.1 wt % HASE-35EO-16C in 0.1 M NaCl filtered and unfiltered with the 0.1 μm filter.

130 nm. If the polymer chains that are derived from the polymerization reaction are cross-linked by the chemical covalent bonds, then such interactions will be irreversible. However, if the aggregates are produced from the association of the hydrophobic groups, which lead to the formation of physical bond, such interactions will be reversible.[1] The physical bonds can be classified as weak or strong physical bonds. The weak physical bonds can be broken and re-formed while the strong physical bonds are stable over the experimental time scale and can only be broken by changing the experimental conditions (e.g., by heating). Examples of weak physical bonds include hydrogen bonds, multiplets in ionomers, and micelles of block or graft copolymers in selective solvents. Examples of strong physical bonds are microcrystals, double and triple helices, and other strong associations that are permanent under the given experimental conditions.

When the aggregates are due to permanent cross-link arising from the synthesis process or strong physical interactions, then it can be removed using a filter with pore size smaller than the size of the aggregates. Wu and co-workers showed that large particles can be removed by filtration.[38,39] The HASE solutions were filtered through a 0.1 μm filter and measured using the DLS. When the 0.1 wt % HASE-35EO-16C sample was forced through the filter, a significant amount of force was required. The distribution functions of 0.1 wt % HASE-35EO-16C after passing through the 0.1 μm filter are shown in Figure 6. From the figure, it is evident that the filtered samples have fairly similar distribution as the unfiltered sample, while the unfiltered sample shows noncontinuous multipeak distribution functions.

The interpretation of the above results is as follows: In the polymer solution, large numbers of associative aggregates are present. The size of the aggregate is larger than 0.1 μm, which makes the filtration difficult. Since hydrophobic groups form reversible junctions, these aggregates are broken during filtration, but they re-form after passing through the filter. The results demonstrate that the association of different polymer chains is temporary or dynamic in nature.

We observe a very small peak in the short relaxation time at measurement angle of 45° for 0.1 wt % HASE solution. It is still unclear on the real meaning of this small peak. In our opinion, there are two possibilities: it is either due to the noise of the correlation function or caused by the internal mode of the polymer aggregate. At short time, the "dead time" of electronics may give rise to an upturn in the correlation function. In that case, the inverse Laplace transformation may yield peaks that have no real physical meaning. The other possibility is that this small peak may be attributed to the internal mode of the large aggregates since we are probing in a regime where the ratio qR_g is larger than 1. On the basis of the DLS theories, the inverse of q possesses the same unit as the wavelength. If qR_g is less than 1, only translational diffusion mode could be detected. If qR_g is larger than 1, internal modes could also be observed at short relaxation times. Brown indicated that for $1 < qR_g < 2$ internal modes, which are q^3-dependent,[36] could be well separated. For $qR_g > 2$, it is difficult to separate the internal modes.[30] The relationship of decay rate and q^3 for HASE in aqueous solutions is difficult to be confirmed due to the scattering of minute quantities of dust at very low angles as it is extremely difficult to completely remove every dust particle in aqueous solution. However, if qR_g is larger than 2, the internal mode will merge with the diffusion mode.

Effect of Polymer Concentrations. By conducting DLS measurements on systems of varying polymer concentrations, the effects of polymer concentrations on the nature of the polymer network structure can be examined. In the present study, more than 10 different concentrations, ranging from very dilute solutions to solutions with concentration close to the overlap concentration regime of HASE-35EO-16C, were prepared in 0.1 M NaCl aqueous solutions neutralized to pH of 9. The overlap concentration, C^*, for the polymer in high salt solutions is approximately 0.5 wt % as determined from the relationship $C^* = 1/[\eta]$. The intrinsic viscosity $[\eta]$ was measured in our laboratory using the U-tube viscometer.[40] The autocorrelation functions obtained at the measurement angle of 45° were analyzed using REPES, and the distribution functions at different concentrations are shown in Figure 7.

From the figure, it is evident that two narrow distributed peaks became three broader distributed peaks when the polymer concentration varies from 0.005 to 0.4 wt %, which means that the distribution of the aggregates becomes broader. Both peaks are similar at the concentration of less than 0.05 wt %. When the polymer concentration is larger than 0.05 wt %, the slow mode shifts to longer relaxation times, which is similar to the trends reported by Alami et al.[41] However, for the fast mode, the peak shifts to shorter relaxation times when the concentration increases from 0.05 to 0.1 wt %. It then shifts to longer times when the concentration exceeds 0.1 wt %.

For the fast and the slow modes, the decay rates and the square of the scattering vector exhibit a linear relationship, indicating that both peaks are attributed to translational diffusion. Table 1 summarizes the diffusion coefficients and the hydrodynamic properties of dilute HASE-35EO-16C in 0.1 M NaCl at pH 9. Figure 8 shows the relationship between the diffusion coefficients and polymer concentrations for the HASE-35EO-16C. For the fast modes, it is evident that the dependence of diffusion coefficient on polymer concentrations in the dilute regime can be separated into two regions with the critical limit at about 0.1 wt %. At $C <$ 0.1 wt %, the diffusion coefficients of the fast mode increase linearly with concentrations. However, at $C >$ 0.1 wt % they decrease with concentration. For the slow mode in dilute solution regime, the diffusion coefficients decrease with increasing concentrations, and the diffu-

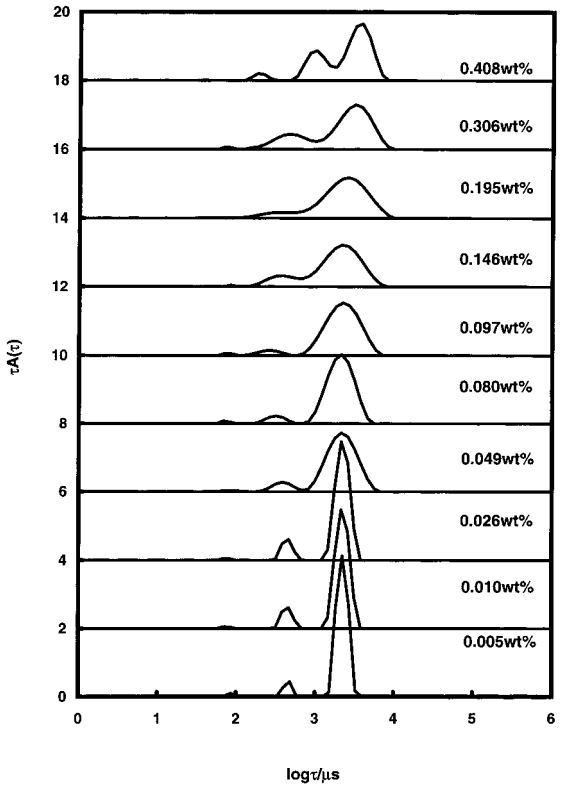

Figure 7. Relaxation time distribution functions of HASE-35EO-16C at different concentrations, at pH 9 and 298 K, in 0.1 M NaCl, at measurement angle of 45°.

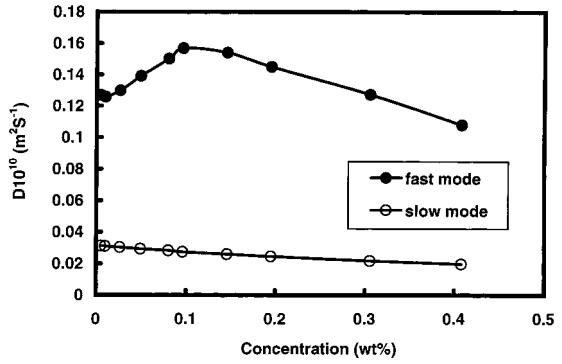

Figure 8. Relationship of diffusion coefficients and concentrations for HASE-35EO-16C at pH 9 and 298 K, in 0.1 M NaCl.

sion coefficients exhibit a linear dependence on the polymer concentrations over the whole dilute solution regime.

Concentration < 0.05 wt %. The region where $C < 0.05$ wt % is designated as the very dilute solution regime. In this region, the diffusion coefficients for the fast process, D_f, and the slow process, D_s, are almost constant, due to the low polymer concentrations; i.e., they are not significantly affected by the interparticle interactions. The two peaks represent the translational diffusion of the unimers and the aggregates or polymer clusters, respectively. Chu et al. observed similar distribution functions for other associative polymer systems in very dilute solutions.[42−44] It cannot be excluded that the fast mode also contains very small clusters or oligomeric aggregates that cannot be distinguished from the unimers. In addition, the aggregate peak (slow mode) is detectable even down to concentration of 0.005 wt %, which suggests that the critical aggregation concentration (cac) for this polymer is very low.

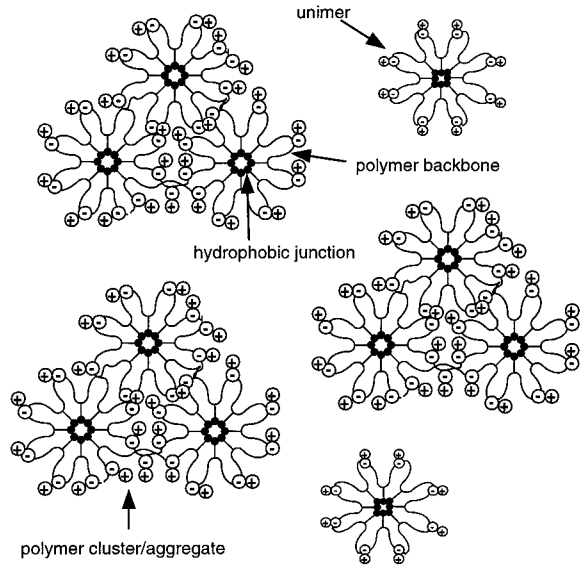

Figure 9. Proposed microstructure of dilute model HASE polymer in 0.1 M NaCl, at pH 9 and 298 K.

By combining the results obtained from static and dynamic light scattering experiments, information on the aggregation number and the conformation of the system can be obtained. Assuming that the dn/dc is approximately the same for both unimer and aggregate species, the intensity ratio of aggregate to unimer as deduced from the REPES analysis (extrapolated to zero scattering angle by taking into account of the particle scattering function for the aggregates at a finite scattering angle) is related to the weight fraction and molar mass of each species in the mixture by the expression

$$\frac{A_{agg}}{A_u} = \frac{(1-x)M_{agg}}{xM_u} \tag{10}$$

where x is the weight fraction of the unimers, and M_u and M_{agg} are the weight-averaged molar masses of unimers and aggregates, respectively. The apparent molar mass (M_T) obtained from static light scattering has contributions from both unimers and aggregates as follows:

$$M_T = xM_u + (1-x)M_{agg} \tag{11}$$

Combining eqs 10 and 11, the number of polymer chains (or unimers) in the aggregates can be determined, where $n = M_{agg}/M_u \sim 5$ and $x \sim 0.35$. Thus, the aggregates formed comprise about five polymer chains with hydrophobes located in the interior and the hydrophilic groups extending to the water in order to satisfy the minimum free energy requirements. The aggregates consisting of five polymer chains are formed by close association, as the diffusion coefficients are independent of concentration. A pictorial representation of the conformations of very dilute HASE in aqueous salt solution is shown in Figure 9.

In this structure, the negative charges are distributed on the outside of the aggregates due to its hydrophilic characteristics. Since the external surfaces of the aggregates contain negative charges, it is difficult for other polymer chains to associate with these aggregates due to the electrostatic repulsion. An equilibrium exists between the hydrophobic and electrostatic interactions.

We postulate that each aggregate contains more than one hydrophobic junction points since the total number of hydrophobes within the aggregate is about 70−80, and the aggregation number per junction should be less than 20−30. Another constraint that prevents the formation of flowerlike micelle with one hydrophobic core is the steric hindrance of the "stiffer" polymer backbone of the polyelectrolyte. Because of the EO spacer and the repulsive force between the charges of the polymer backbone, the aggregates exhibit a larger radius of gyration and hydrodynamic radius.

As reported by Chu et al.,[42] two different methods can be used to estimate the average radius of gyration of the aggregates $R_{g,agg}$. One is based on the equation

$$\langle R_g^2 \rangle_z = \frac{xM_u R_{g,u}^2 + (1-x)M_{agg} R_{g,agg}^2}{xM_u + (1-x)M_{agg}} \qquad (12)$$

The other is to subtract the flat background scattering of single coils to obtain the scattering that is solely due to the aggregates by using the intensity ratio determined from dynamic light scattering measurements. On the basis of the two methods, the R_g of the aggregates is estimated to be about 145 nm. From eq 9, the hydrodynamic radius of unimers and aggregates are 19 and 80 nm, respectively. The apparent hydrodynamic radii of the unimers and aggregates are listed in Table 1. The ratio of R_g/R_h is larger than 1.5 with a mean value of 1.8. This value supports the description that the aggregate is a draining coil. The fractal dimension listed in Table 1 reveals that its magnitude does not change with polymer concentration over this concentration regime. For a d_f value of 2.35, it implies that the structure is compact. The apparent R_h of the unimer and aggregate and the ratio between these two radii are summarized in Table 1. $R_h(agg)/R_h(u)$ is ~ 4 at $c < 0.05$ wt % and increases to ~ 6 at c of 0.5 wt %. This corresponds to the static fractal dimension that decreases with concentration, suggesting that the aggregates are less compact at higher polymer concentrations.

0.05 wt % < C < 0.1 wt %. When the polymer concentrations increase from 0.05 to 0.1 wt %, the diffusion coefficients for the fast mode increase linearly with polymer concentrations. As discussed by Brown,[30] the diffusion coefficient determined at a finite concentration is characterized by the concentration coefficient, k_D, given by

$$D = D_0(1 + k_D C + ...) \qquad (13)$$

where D_0 is the diffusion coefficient at infinite dilution, k_D is the second virial diffusion coefficient, C is the polymer concentration, and D is the diffusion coefficient at finite concentration C. The interrelation between k_D and k_f in terms of A_2 can be expressed by

$$k_D = 2A_2M - k_f - v_2 \qquad (14)$$

where k_D is determined directly from DLS, A_2 from static light scattering, k_f from pulsed-field-gradient NMR and v_2, which is the partial specific volume. From the plot of D vs C, as shown in Figure 8, the slope of the graph gives the magnitude of k_D of the unimers, which can be used to interpret the polymer/solvent interaction. When the polymer concentration increases, the polymer/solvent interaction should increase, giving rise to higher diffusion coefficients. The results are similar to the behavior of many polymers in good solvents. The positive value of k_D implies that the polymer/solvent interaction is larger than the polymer/polymer interaction. At this condition, the fast mode is also caused by the translational diffusion of the unimers. The intercept of the plot is the diffusion coefficient at infinite dilution, which can be used to calculate the hydrodynamic radius. If the polymer concentration is low enough, the effect of polymer concentrations is negligible, yielding a diffusion coefficient that is independent of concentration.

Unlike the fast mode, the diffusion coefficients of the slow modes decrease linearly with increasing polymer concentrations over the dilute solution regime (i.e., 0.05−0.4 wt %). This result is similar to the previous study on combed polymers reported by Winnik and coworkers.[45] This decrease may be attributed to two factors: (1) The second virial diffusion coefficient of the cluster, k_{D^-} the negative value of k_D implies that the polymer/polymer interaction for the aggregates is significant. (2) The restructuring of aggregates in this concentration regime, the fractal dimension, d_f, decreases from 2.11 to 1.90. This implies that the structure of the aggregates becomes more open (i.e., less compact). From eq 4, it can be conjectured that with the decrease of d_f the radius of the aggregate will increase, resulting in the decrease of the diffusion coefficient and hence the corresponding increase in the solution viscosity. The reduced diffusion coefficients are calculated by correcting the effect of viscosity on the diffusion coefficient. These reduced values are shown in Table 1. It is obvious that the values of $(D\eta/T)$ for the slow mode at all concentrations are fairly similar. This means that the decrease in the diffusion coefficients is attributed to the increase in the solution viscosity.

0.1 wt % < C < 0.4%. In this concentration regime, the diffusion coefficients for both the fast and slow modes decrease linearly with increasing polymer concentrations. The reason for the decrease in the diffusion coefficients for the slow mode is due to the higher solution viscosity as previously discussed. No transition is observed for the slow mode at concentration 0.1 wt %, indicating that there is no significant structural change in the aggregates. However, a sharp transition is observed for the fast mode at concentration 0.1 wt %, implying that the conformation of the unimers undergoes a sharp transition.

The macroscopic viscosity was used to calculate the reduced diffusion coefficients for the fast mode. These values are shown in Table 1. From the table, it is obvious that the values of $(D\eta/T)$ for the fast mode are not identical. This suggests that the decrease in the diffusion coefficients does not correspond to the viscosity increase. It is related to the structural change of the unimers. With increasing polymer concentration, the correlation length between two polymer chains would decrease until it reaches a critical value where the hydrophobes from different polymer chains associate to form oligomers. Beyond 0.1 wt %, the unimers no longer exist as they are converted to dimers or trimers. This is consistent with the decrease in the fractal dimension, signifying that the oligomers are less compact than the unimers.

Conclusions

The hydrophobically modified alkali soluble emulsion, HASE-35EO-16C, in 0.1 M NaCl aqueous solutions at

pH 9, 298 K, was studied using static and dynamic light scattering techniques. Two peaks in the distribution function are observed; the fast peak corresponds to the diffusion of unimers at very dilute solutions. The slow mode is attributed to the diffusion of aggregates. This aggregate is formed by the weak physical interactions associated with hydrophobic forces. The aggregate comprised of about five single polymer chains coexists with the unimers. Inside the aggregates, there are more than one micellar junction centers with the hydrophilic backbone extended to the water environment. From the fractal dimension analysis, the aggregates become less compact as concentration increases.

Acknowledgment. The authors acknowledge the support and enthusiasm of Dr. Dave Bassett in the research collaboration between NTU and Union Carbide. We also acknowledge the financial support provided by the NSTB-Ontario Joint Collaborative Grant Scheme and the Ministry of Education. In addition, we thank Professor Wyn Brown, Professor Mitch Winnik, and Mr. Ng Wei Kiat for their helpful suggestions. We thank the reviewers for their constructive comments.

References and Notes

(1) Rubinstein, M.; Dobrynin, A. V. *TRIP* **1997**, *5*, 181.
(2) Schultz, D. N.; Glass, J. E. *Polymers as Rheology Modifiers;* ACS Symposium Series Vol. 462; American Chemical Society: Washington, DC, 1991.
(3) Calbo, L. J. *Handbook of Coating Adhesives;* Marcel Dekker: New York, 1993; Vol. 2.
(4) Nystrom, B.; Walderhaug, H.; Hansen, F. K. *J. Phys. Chem.* **1993**, *97*, 7743.
(5) Winnik, M. A.; Yekta, A. *Curr. Opin. Colloid Interface Sci.* **1997** *2*, 424.
(6) Volpert, E.; Selb, J.; Candau, F. *Polymer* **1998**, *39*, 1025.
(7) Alexandridis, P. *Curr. Opin. Colloid Interface Sci.* **1996**, *1*, 490.
(8) Walderhaug, H.; Nystrom, B. *Trends Phys. Chem.* **1997**, *6*, 89.
(9) Goldmints, I.; Holzwarth, J. F.; Smith, K. A.; Hatton, T. A. *Langmuir*, **1997**, *13*, 6130.
(10) Jorgensen, E. B.; Hvidt, S.; Brown, W.; Schillen, K. *Macromolecules* **1997**, *30*, 2355.
(11) Tam, K. C.; Jenkins, R. D.; Winnik, M. A.; Bassett, D. R. *Macromolecules* **1998**, *31*, 4149.
(12) Lairez, D.; Adam, M.; Carton, J. P.; Raspaud, E. *Macromolecules* **1997**, *30*, 6798.
(13) Kjoniksen, A.; Nystrom, B.; Iversen, C.; Nakken, T.; Palmgren, O.; Tande, T. *Langmuir* **1997**, *13*, 4948.
(14) Iversen, C.; Kjoniksen, A.; Nystrom, B.; Nakken, T.; Palmgren, O.; Tande, T. *Polym. Bull.* **1997**, *39*, 747.
(15) Khougaz, K.; Astafieva, I.; Eisenberg, A. *Macromolecules* **1995**, *28*, 7135.
(16) Zhou, Z.; Chu, B.; Nace, V. M. *Langmuir* **1996**, *12*, 5016.
(17) Scahller, E. J.; Sperry, P. In Calbo, L. J. *Handbook of Coating Additives;* Marcel Dekker: New York, 1992; Vol. 2.
(18) Jenkins, R. D.; Delong, L. M.; Bassett, D. R. In *Hydrophilic Polymers: Performance with Environmental Acceptability*; Glass, J. E., Ed.; Advances in Chemical Series 248; American Chemical Society: Washington, DC, 1996; p 425.
(19) Guo, L.; Tam, K. C.; Jenkins, R. D. *Macromol. Chem. Phys.* **1998**, *199*, 1175.
(20) Guo, L. Master Dissertation, Nanyang Technological University, Singapore, 1997.
(21) Tirtaatmadja, V.; Tam, K. C.; Jenkins, R. D. *Macromolecules* **1997**, *30*, 3271.
(22) Tirtaatmadja, V.; Tam, K. C.; Jenkins, R. D. *Macromolecules* **1997**, *30*, 1426.
(23) English, R. J.; Gulati, H. S.; Jenkins, R. D.; Khan, S. A. *J. Rheol.* **1996**, *41*, 427.
(24) Kumacheva, E.; Rharbi, Y.; Winnik, M. A.; Guo, L.; Tam, K. C.; Jenkins, R. D. *Langmuir* **1997**, *13*, 182.
(25) Ng, W. K.; Tam, K. C.; Jenkins, R. D. *Eur. Polym. J.* **1999**, *35*, 1245.
(26) Tirtaatmadja, V.; Tam, K. C.; Jenkins, R. D. *AIChE J.* **1998**, *44*, 2756.
(27) Horiuchi, K.; Rharbi, Y.; Spiro, J. G.; Yekta, A.; Winnik, M. A.; Jenkins, R. D.; Bassett, D. R. *Langmuir* **1999**, *15*, 1644.
(28) Horiuchi, K.; Rharbi, Y.; Yekta, A.; Winnik, M. A.; Jenkins, R. D.; Bassett, D. R. *Can. J. Chem.* **1998**, *76*, 1779.
(29) Dai, S.; Tam, K. C.; Jenkins, R. D. *Macromol. Chem. Phys.*, accepted.
(30) Brown, W. *Dynamic Light Scattering- the Method and Some Applications;* Clarendon Press: Boston, 1993.
(31) Flory, P. J. *Principles of Polymer Chemistry;* Connell University Press: London, 1953.
(32) Chu, B. *Laser Light Scattering-Basic Principles and Practice*, 2nd ed.; Academic Press: Boston, 1991.
(33) Islam, M. F.; Jenkins, R. D.; Ou-Yang, H. D.; Bassett, D. R., submitted for publication.
(34) Nicolai, T.; Durand, D.; Gimel, J. C. In *Light Scattering-Principles and Development;* Brown, W., Ed.; University Press: Oxford, 1996.
(35) Carpinti, M.; Ferri, F.; Giglio, M.; Paganini, E.; Perini, U. *Phys. Rev. A* **1990**, *42*, 7347.
(36) Raspaud, E.; Lairez, D.; Adam, M.; Carton, J. P. *Macromolecules* **1994**, *27*, 2956.
(37) Brown, W. *Light Scattering- Principles and Development;* University Press: Oxford, 1996.
(38) Siddiq, M.; Wu, C.; Li, B. *J. Appl. Polym. Sci.* **1996**, *60*, 1995.
(39) Siddiq, M.; Li, B.; Wu, C. *J. Polym. Sci., Part B: Phys.* **1997**, *35*, 89.
(40) Ng, W. K. Private communication.
(41) Alami, E.; Almgren, M.; Brown, W.; Francois, J. *Macromolecules* **1996**, *29*, 2229.
(42) Zhou, Z.; Peiffer, D. G.; Chu, B. *Macromolecules* **1994**, *27*, 1428.
(43) Zhou, Z.; Chu, B.; Nace, V. M. *Langmuir* **1996**, *12*, 5016.
(44) Zhou, Z.; Yang, Y.; Booth, C.; Chu, B. *Macromolecules* **1996**, *29*, 8357.
(45) Xu, B.; Li, L.; Zhang, K.; Macdonald, P. M.; Winnik, M. A. *Langmuir* **1997**, *13*, 6896.

MA990887N